Research Article

Ye Wu and Yun Wan*

The low-velocity impact and compression after impact (CAI) behavior of foam core sandwich panels with shape memory alloy hybrid face-sheets

https://doi.org/10.1515/secm-2019-0034
Received Aug 19, 2019; accepted Sep 22, 2019

Abstract: Due to the properties of shape memory effect and super-elasticity, shape memory alloy (SMA) is added into glass fiber reinforced polymer (GFRP) face-sheets of foam core sandwich panels to improve the impact resistence performance by many researchers. This paper tries to discuss the failure mechanism of sandwich panels with GF/epoxy face-sheets embedded with SMA wires and conventional 304 SS wire nets under low-velocity impact and compression after impact (CAI) tests. The histories of contact force, absorbed energy and deflection during the impact process are obtained by experiment. Besides, the failure modes of sandwich panels with different ply modes are compared by visual inspection and scanning electron microscopy (SEM). CAI tests are conducted with the help of digital image correlation (DIC) technology. Based on the results, the sandwich panels embedded with SMA wires can absorb more impact energy, and show relatively excellent CAI performance. This is because the SMA wires can absorb and transmit the energy to the outer region of GFRP face-sheet due to the super-elasticity-behavior. The failure process and mechanism of the CAI test is also discussed.

Keywords: Hybrid sandwich structures; Shape memory alloy; Low-velocity impact; Compression after impact; Failure mechanism

1 Introduction

Due to the high physical and mechanical properties in term of high specific strength and stiffness, sandwich panels are being widely applied in various branches of engineering fields, including leading applications such as the aircraft, civil engineering and railway industries [1–6]. The sandwich panels with carbon fiber reinforced plastic (CFRP) face-sheets exhibited better mechanical performance lower weight compared to those with metal face-sheets [7–9]. However, because of the poor toughness of the fiber reinforced plastic face-sheets, the face-sheets can be easily perforated due to the sandwich structures is sensitive to impact loading. Meanwhile, barely visible damage after low energy impact could lead to a significant reduction to the structural load bearing capability. The compressive strength of the sandwich structure can be reduced up to 50% after an impact event [10–12]. Although the impact damage is nearly invisible, such damage could lead to sharp reduction to the structural load-bearing capability, possibly causing catastrophic failure of the sandwich structure. Thus, the study on the low-velocity impact failure mechanism and CAI behavior of sandwich panels is deserved more attention. It is essential to study the damage mode of the sandwich structure with composite face-sheets, and it is necessary to investigate the compression after impact (CAI) behavior of sandwich composite panels.

Based on previous research, the residual after impact has been adopted to evaluate the impact resistance of sandwich structures with different facesheets and core materials [12–15]. Two types of sandwich panels which are based on hybrid cores consisting of polymer resin reinforced by metallic millitubes have been developed and characterize by Ji [11]. The damage mechanism of sandwich panels with thin aluminum skins and a Nomex™honeycomb core under impact and CAI have been presented by Gilioli [13]. Giannopoulos [14] presented the interrogation of low-velocity impact and compression

***Corresponding Author: Yun Wan:** School of Civil Engineering and Architecture, East China Jiaotong University, Nanchang, China; Email: address:wanyun0505@163.com; Tel./fax: +86-791-87046046
Ye Wu: Jiangxi Province Key Laboratory of Hydraulic and Civil Engineering Infrastructure Security, School of civil and architecture engineering, Nanchang Institute of Technology, Nanchang, China

after impact test results on a woven fiber composite having a fire retardant, syntactic core, two phase epoxy matrix. The main failure modes of sandwich panels under impact load including face-sheet failure, matrix/core crush and interface delamination. It is evident that the face-sheet play an important role on the performance of sandwich panels under the impact load. Moreover, tough face-sheet could reduce the level of destruction in the internal structure including core material and interface delamination.

In order to improve the impact resistence performance of composite face-sheet, researchers have carried out some works. Research indicates that carbon fiber has excellent mechanical properties, but a relatively poor impact resistence performance compared to the glass/aramid fiber. This is due to the rigidity and fragility of the carbon fiber [16]. The influence of the matrix properties, type of fiber and fiber orientation on low-velocity impact behavior of the fabric reinforced hybrid composites with stratified filled epoxy matrix was investigated [17]. Reference [18] reported that high angle between neighboring layer increased the delamination area under the low-velocity impact. Liu *et al.* [19] designed a new type of hybrid laminate with five layers of woven carbon and unidirectional carbon fibers. In general, there are two main kinds of methods to improve the impact resistence performance of composite face-sheet of sandwich, hybrid reinforced fiber and lay-up designs. However, the low impact resistance is hard to improve fundamentally due to the fragility and rigidity of matrix and common fiber.

Compared to fiber reinforced plastic, metal has an excellent low-velocity impact performance due to its high ductility. Aluminium was added into fiber reinforced plastic to improve the performance of impact in aerospace field [20]. Moreover, steel wire nets are employed to improve the impact resistence performance of concrete slab [21–23]. In the civil engineering, steel wire nets are widely used in concrete-shotcrete. It is reported that [21] the use of fiber reinforcement in concrete/shotcrete can greatly enhance the punching shear capacity, flexural ductility and toughness. Reference [22] shows that the use of high-performance polypropylene fiber reinforcement in shotcrete, with sufficient fiber content, can greatly improve flexural ductility, toughness, and ultimate load capacity. Therefore, it can be used with steel mesh and steel fiber reinforcement, especially in tunnel applications. The experimental and numerical works conducted by Liu *et al.* [23] indicate that the steel wire nets enhance the toughness of concrete. Therefore, the metal wire nets can be a candidate to improve the impact resistence performance of conventional fiber reinforced plastic. Because of the properties of high failure strain, superelastic and shape recoverable, shape memory alloy (SMA) has been added into the composite laminates to improve the low-velocity performance in many papers [24–27]. The impact response of composite laminates embedded with SMA wires in the thermal environment was investigated by Shariyat [24]. The effect of embedding SMA wires on the impact behavior of composite beam under different mass and initial incident energies was studied by Khalili [25] studied into the laminated composite beam on the impact behavior of the beam with different masses and initial incident energy. Eslami-Farsani [26] investigated the high-velocity impact behavior of composite laminates enhanced with SMA wires. In their works, the influences of volume fraction and pre-strain of SMA wires on the impact responses of composite laminates was investigated. However, based on the authors' knowledge, there is less attention paid to the advantages of SMA wires compared to the convention 304 SS wires in improving the impact resistance of composite laminates.

In this paper, low-velocity impact and CAI experiments are conducted to analyze the impact resistence performance of foam core sandwich panels with SMA hybrid GF/epoxy face-sheets which are designed with different orientations and numbers of SMA wires. In order to present the advantage of the sandwich panel hybrid with SMA wires, similar sandwich panels embedded with 304 SS wire nets are fabricated and the impact resistance is compared with the sandwich panels with SMA wires. The Instron/9250 HV low-velocity impact device is employed and the impact responses including contact force-time, absorbed-time and defection-time curves are recorded. Moreover, macro and micro failure morphology of sandwich panels with different ply modes are presented and compared. Digital image correlation (DIC) is used to assist to analyze the failure mechanism of designed sandwich panels during CAI tests. Finally, the advantage of SMA enhanced sandwich panels in CAI tests are presented and some conclusions explained this results are drawn.

2 Experimental details

2.1 Materials and manufacturing

As shown in Figure 1, the test specimens are fabricated by vacuum assisted resin infusion (VARI). Vinyl ester resin which can be cured at room temperature mixed with hardening and accelerating agent was employed as the matrix. The main of hardening and accelerating agents were Methyl Ethyl Ketone Peroxide (MEKP) and Dimethylani-

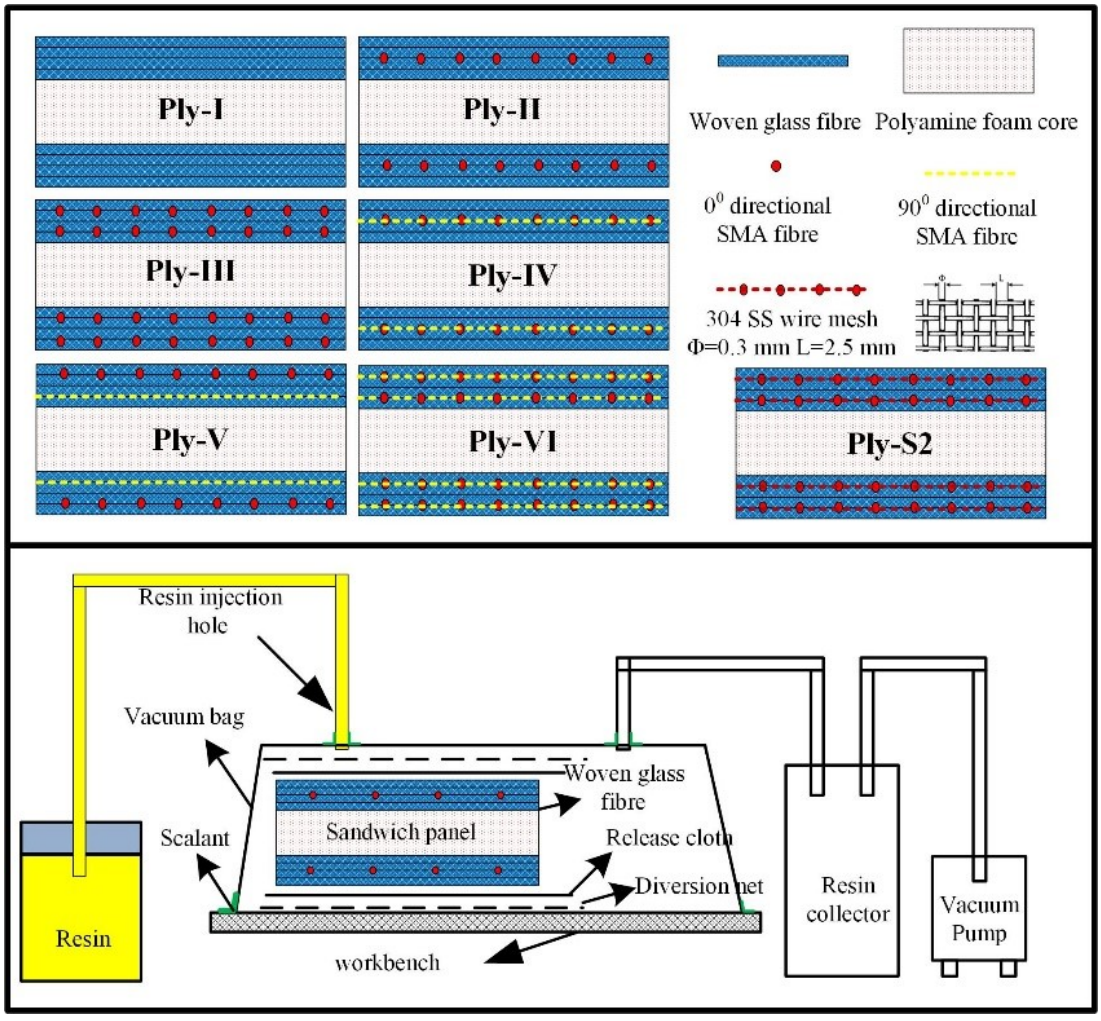

Figure 1: Ply modes of different foam-core sandwich panels and the schematic diagram of VARI

line. Matrix, accelerator and hardener were mixed at mass ratio of 100: 1.0: 0.1. Two-dimensional orthogonal plain woven glass fiber fabric with a surface a density of 300 g/m^2 and single layer thickness of 0.3 mm was used as reinforced fibers. The compressive modulus and strength of the foam core with a density of 75 kg/m^3 are 12 MPa and 0.5 MPa. A commercially available NiTi alloy with a diameter of 0.3 mm was purchased from PeierTech, Jiangyin, China, and the mass fraction of Ni in the alloy is 55.97%. The mechanical properties of the same SMA wire were tested by Li [28].

2.2 Low-velocity drop weight impact test

Instron /9250 HV low-velocity impact device is employed to carry out the drop-weight experiment at room temperature. As shown in Figure 1, the specimens with dimension of 100 mm × 100 mm were clamped by pneumatic press fixture. A circle area with a radius of 38.1 mm was located at the central area of the specimens. A hemispherical impactor with weight of 17.2 kg and a diameter of 12.7 mm was adopted in all tests. During the impact process, a load cell located at the above of the impactor bar was used to measure the contact force. The work of data storage and analysis was completed with the help of computer and software. Then, the impact history of absorbed energy and deflection were presented as well. In this paper, all type of specimens were tested at the incident energy of 14 J, 18 J and 22 J, respectively. For each type of ply codes under the same incident energy, the experiment was repeated three times.

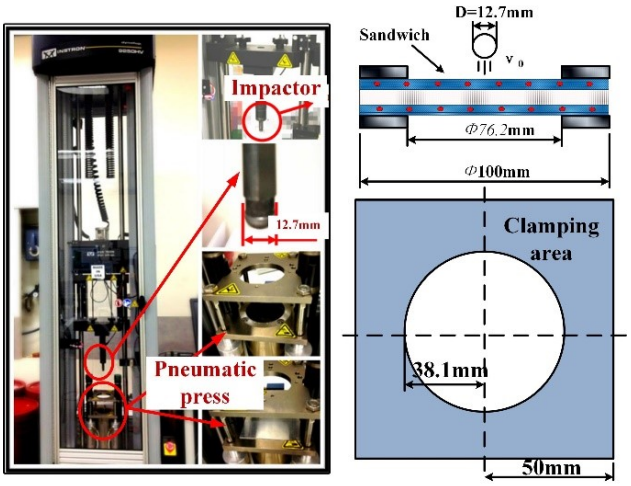

Figure 2: Low-velocity impact test set-up and illustration of the samples

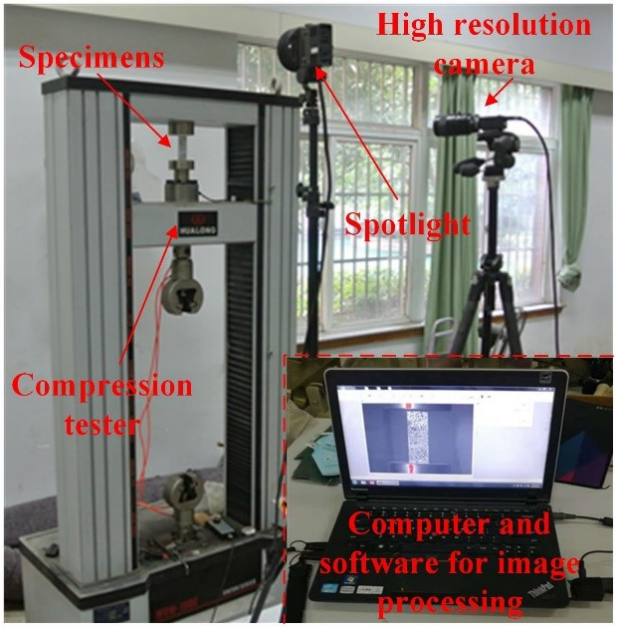

Figure 3: Set-up of compressive test and DIC device

2.3 Compression test after low-velocity impact

CAI tests are conducted to evaluate residual performance of the impacted sandwich panels with different ply codes based on ASTM D7137 standard [29]. This is because of the foam core/facesheet delamination and the facesheet failure induced by low velocity impact can make a significant reduction on the compressive strength of sandwich panels [30, 31]. The set-up of the compressive test is shown in Figure 2. During the compressive test, the speed of 0.25mm/min was set to the load cross beam. Meanwhile, a 2-D digital image correlation (DIC) system was build up to measure and record the strain of the face-sheet. As shown in Figure 3, the DIC system is consist of specimen marked with white base and blackspot on one face-sheet, high-resolution camera, spotlight and computer with analysis software.

2.4 Characterization technique

In order to analyze the failure mechanism of the sandwich panels with different ply code, visual inspection and scanning electron microscopy (SEM, Hitachi S-4300, Tokyo, Japan) were employed to observe failure modes such as fiber broken, matrix crush and delamination. Damage region including SMA wire is our main concern. This is because the performance of interface region could indicate the enhancement mechanism of the new type of hybrid sandwich panels.

3 Results and discussions

This study focuses on the impact response of sandwich panels consisting of seven different modes of face-sheets. Impact energy were chosen as 14, 18 and 22J.

3.1 Low-velocity impact response history of the designed hybrid sandwich panels

In Figure 4-6, contact force-time curves of different configurations for 14, 18 and 22J impact energies are presented, respectively. From the figures, it can be seen that contact force history of each ply mode shows a similar process under different incident energies. Figure 4 reveals that the maximum contact force increases with the adding of SMA in the hybrid composites. For example, the maximum contact force of ply I and VI under the incident energy of 14 J is 1.97 kN and 2.76 kN, respectively. And, for incident energies of 14J, 18J and 22J, the maximum contact force of ply VI shows an improvement of 40.1%, 37.7% and 27%, relative to ply I, respectively. For ply I, when the contact force is up to the maximum, it decreases sharply and the plates lose the load bearing capacity. Though second peak contact force was obtained soon, the value of second peak contact force increased sharply. However, two peak values of the contact force are observed in the contact force-time curves of the hybrid composites. This phenomenon indicates that hybrid sandwich panels can absorb considerable impact

Table 1: The key values of the impact response and the increase to the ply mode I for the incident energies of 18J and 22J

Incident Energy	Ply Mode	First Peak Force / kN	Increase / %	Second Peak Force / kN	Increase / %	Time interval between two peak force / ms	Maximum Displacement / mm	Increase / %
18J	I	2.07	–	1.80	–	17.59	22.30	–
18J	VI	2.85	37.68	2.85	58.33	2.55	10.00	−55.16
18J	S2	2.90	40.10	2.79	55.00	0.29	11.02	−50.58
22J	I	2.26	–	2.32	–	15.59	21.47	–
22J	VI	2.87	27.00	2.62	12.93	3.87	12.82	−40.29
22J	S2	2.88	27.43	2.78	19.83	0.62	14.51	32.42

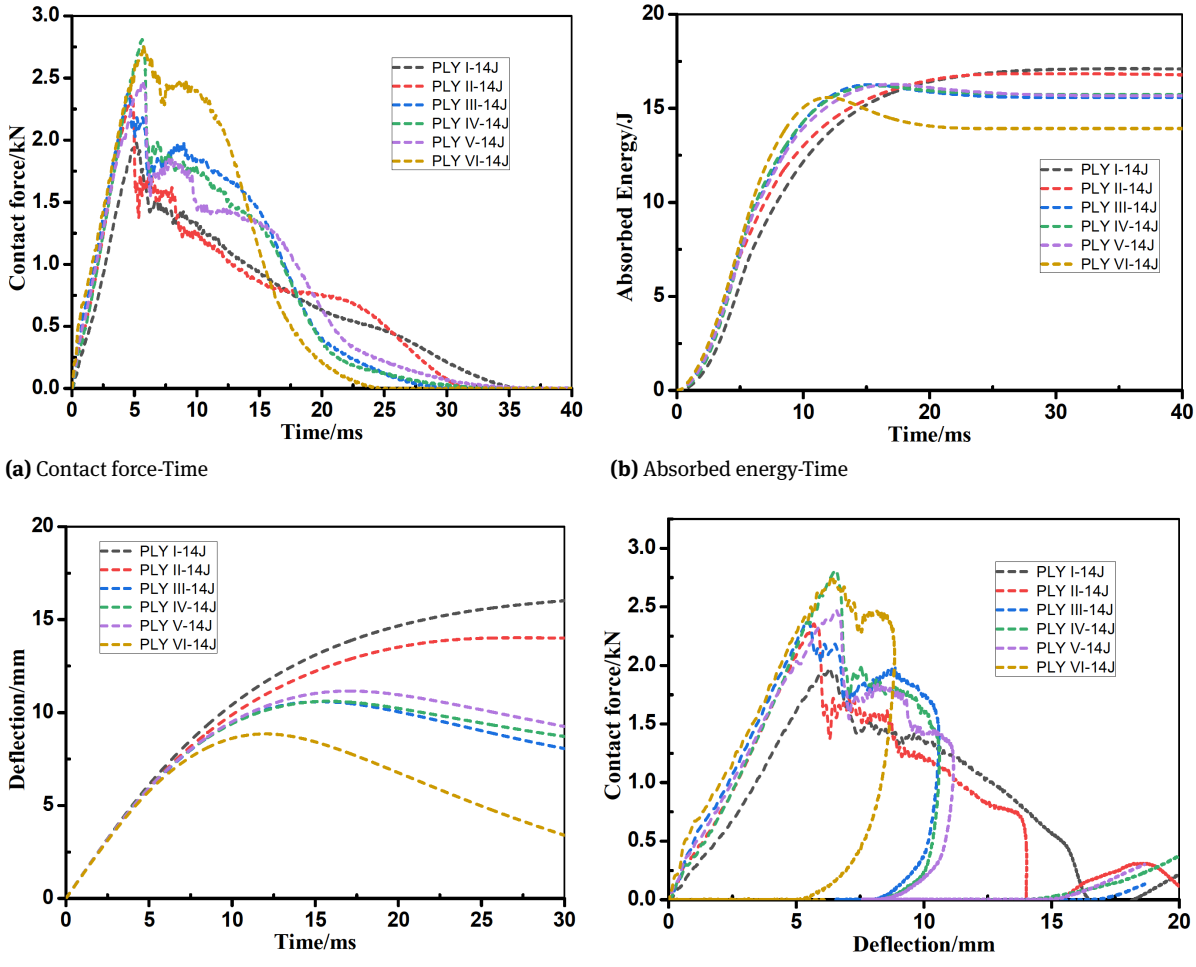

(a) Contact force-Time

(b) Absorbed energy-Time

(c) Deflection-Time

(d) Contact force-Deflection

Figure 4: Comparisons of impact responses between different ply code under incident energy of 14J

energy sustainably after the contact force reaching the peak value. Thus, the impact resistance performance is improved by inserting SMA wires into the GFRP. This is because of the contact force of hybrid sandwich panels keeps a large level for a longer time than the sandwich with GFRP face-sheets.

Figure 7 shows typical impact responses among the sandwich panels with different face-sheets under incident energies of 18J and 22J. Besides, the key values extracted from the experimental results are summarized in Table 1. In general, there are two peak contact forces during the impact process for all samples. Besides, comparing to the

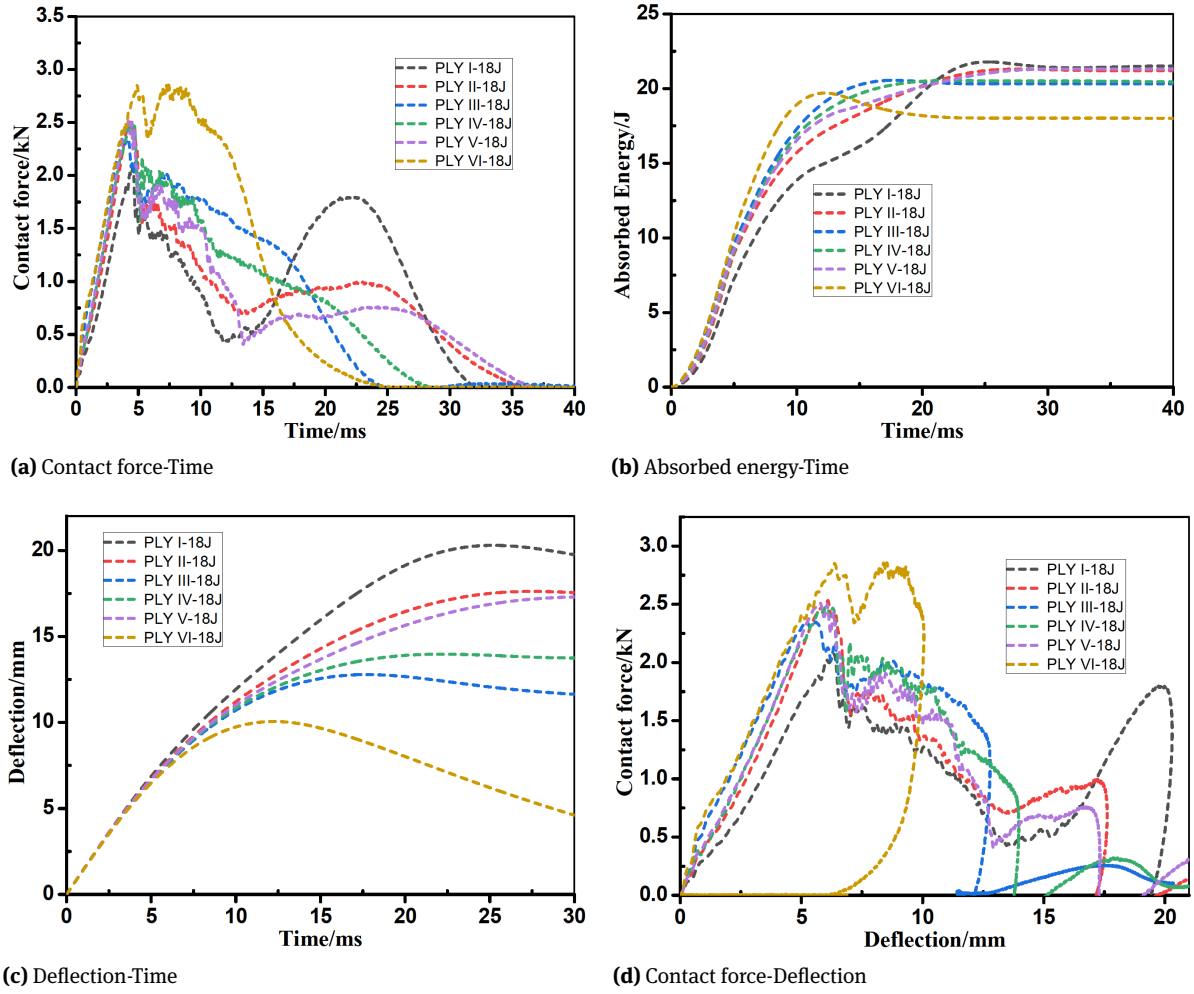

(a) Contact force-Time

(b) Absorbed energy-Time

(c) Deflection-Time

(d) Contact force-Deflection

Figure 5: Comparisons of impact responses between different ply code under incident energy of 18J

conventional laminate, the similar peak value of the contact force of Ply VI and S2 increases signally with the help of SMA and 304 SS wire net. Secondly, for Ply I impacted under the incident energy of 18 J, the contact force reaches the peak value twice in 22.3 ms. However, for Ply VI and Ply S2, the sandwich with hybrid face-sheet, two peak values of contact force appear during a shorter time interval of 2.55 ms and 0.29 ms. It indicates that the Ply VI sandwich can keep high value of contact force for a longer time than Ply S2. This is attribute to the superelastic property of SMA. Thus, Ply VI sandwich can absorb more impact energy. As shown in Figure 7, there are two peak forces shown in the contact force-time curve of Ply I. It is due to the impactor penetrates the upper face-sheet and resulting in damages the bottom face-sheet as well. However, for Ply VI and Ply S2, two peak forces are cause by the failure of GFRP and SMA/ 304 SS with relative high ductility. Moreover, in terms of the rebound energy of Ply VI and S2, the impactor rebounds before the impactor penetrates the upper face-sheet.

3.2 Failure mechanism of different types of sandwich panels under low-velocity impact with various incident energies

The impact damage morphology of different types of hybrid sandwich panels are presented in Figure 8. In general, the impact damage shows a circle shape in both two sides of the sandwich panels. With the addition of SMA and 304 SS wire net, there is less damage area on the front and rear face-sheet under the same incident energy. As shown in Figure 8, a yellow circle with the same diameter as the impactor separates the damage and intact region. And the failure region for both upper and bottom surfaces of ply code I is concentrated in a circular region, besides, the di-

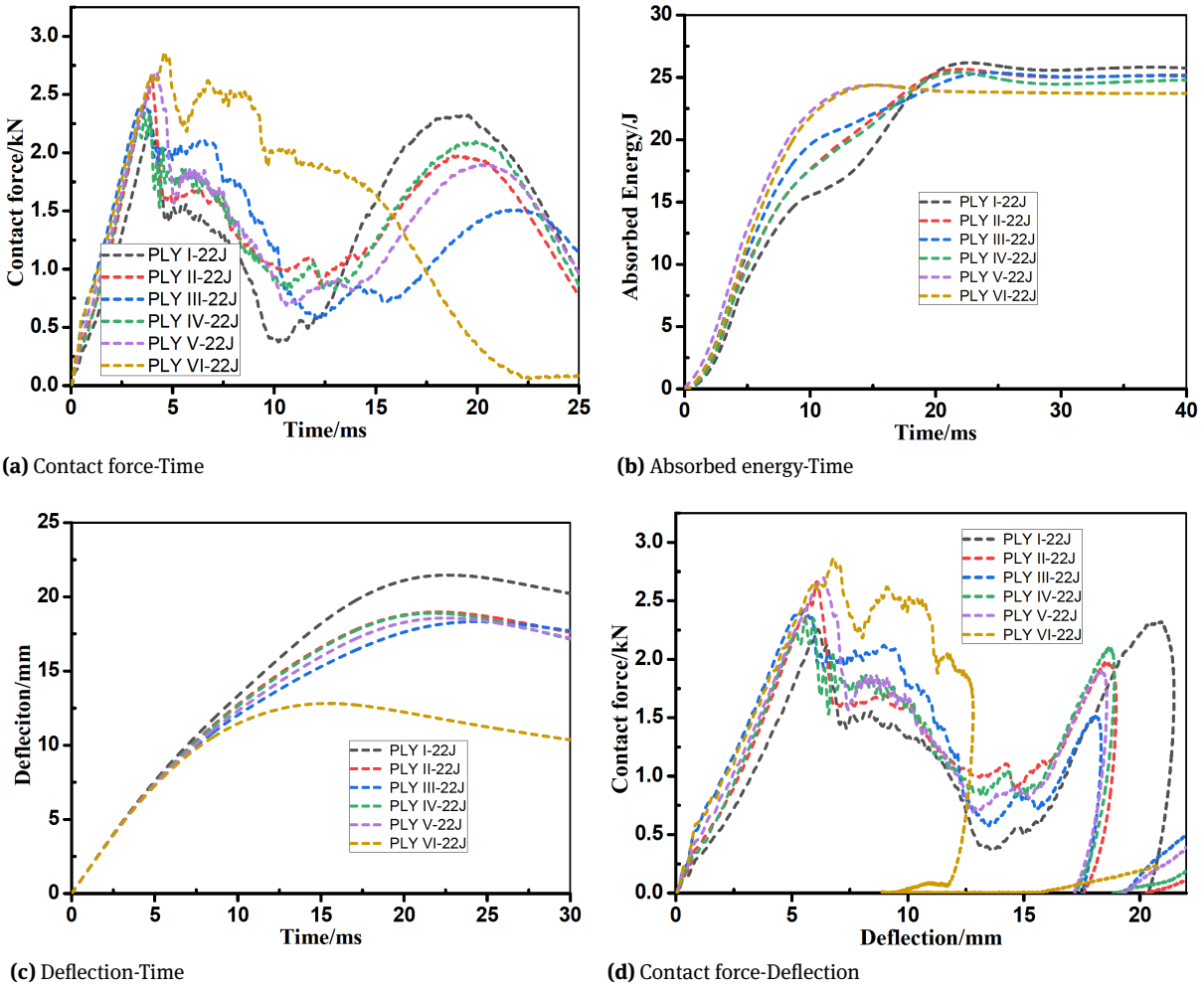

(a) Contact force-Time

(b) Absorbed energy-Time

(c) Deflection-Time

(d) Contact force-Deflection

Figure 6: Comparisons of impact responses between different ply code under the incident energy of 22J

ameter of upper damage region is approximately equal to the size of the impactor for the impact energy of 22J. But for Ply II-VI and Ply S2, there is significant incomplete damaged region located between the central failure region and the outside intact face-sheet. Moreover, there is more incomplete damaged region on the impact faces of Ply II-VI relative to Ply S2. This phenomenon indicates that more face-sheet region is damaged and more impact energy is dissipated with the addition of SMA and 304 SS wire net. This is because of the high elongation of 304 SS and SMA absorbs and transmit the impact energy from the center to the outer region of face-sheets.

The typical cross sections of low-velocity impact cases is shown in Figure 9. Shipsha's results [32] indicated that the typical damage morphology for foam-core sandwich panels under low-velocity impact mainly includes delamination at the interface, broken fiber, partial crushed core located around the impactor and the permanent indentation on the upper face-sheet. All four types of failure modes can be seen clearly for each Ply code in Figure 9. For Ply I, with increasing of the incident energy, there is no significant difference in the damage of front face-sheet among the cases with different incident energy, and, the foam core crushed and expands to the rear face-sheet. However, for Ply II-VI, the foam core and bottom face-sheet are both protected better and show no large difference among different Ply codes relative to Ply I. Besides, with the increasing of incident energies, the degree and scale of damage for upper face-sheet become worse. This phenomenon indicates that the face-sheet embedded with SMA can absorb more impact energy due to hyperelastic behavior. In terms of the orientation and number of embedded SMA, the fracture morphology of Ply III-V, enhanced with more numbers of SMA wire layers, is similar. Generally, the face-sheet enhanced with more layer number of SMA could be more intact under the same incident energy.

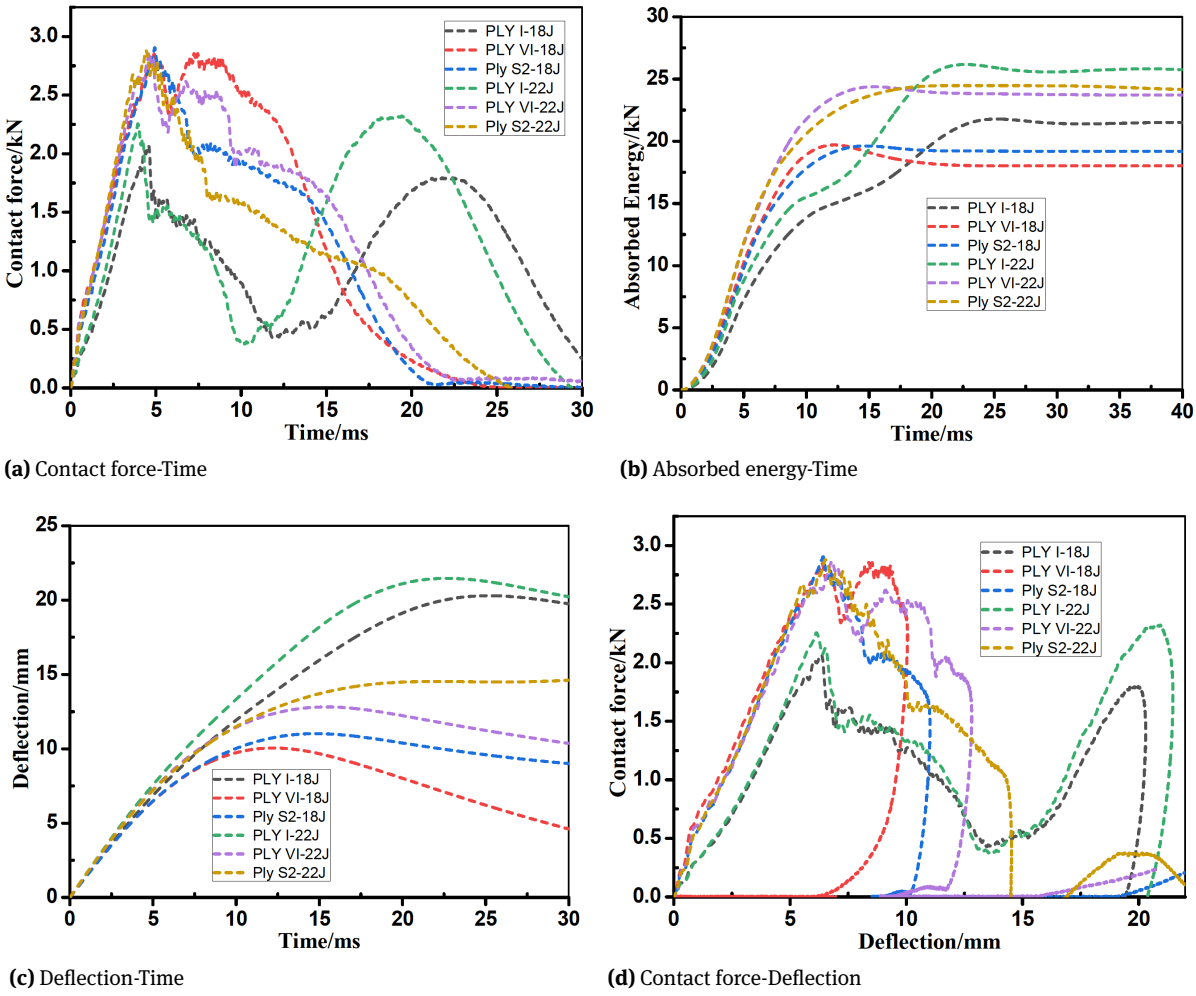

(a) Contact force-Time

(b) Absorbed energy-Time

(c) Deflection-Time

(d) Contact force-Deflection

Figure 7: Comparisons of impact responses between the sandwich panels with different face-sheets under the incident energy of 18J and 22J

Under the impact energy of 18 J, typical cross-section fracture morphology of Ply I, VI and S2, the GFRP face-sheets hybrid with nothing, two layers orthogonality SMA wire and 304 SS wire nets, are compared in Figure 10. For Ply I, the central region of upper face-sheet was completely destroyed during the impact event. But for Ply S2, there is an obviously permanent indentation in the central region, and the fiber and matrix are relatively intact. This is due to the 304 SS wire nets absorbing more impact energy with the property of high elongation. Besides, the fiber breaking and the plastic deformation of 304 SS wire nets lead to the central permanent indentation. However, for Ply VI, the impact of permanent indentation shows not obviously. Moreover, there is more crushed core located around the impact central region and a continuous gap between the upper face-sheet and the crushed core can be observed. Thus, during the low-velocity process, the characteristic of hyperelastic and shape memory of SMA resulted in more core was compress crushed and the deformation recovery, and then, created the continuous gap.

Typical microstructure damage aroud the impact region of the SMA hybrid sandwich panels is shown in Figure 11 and the damage morphology of the SMA hybrid face-sheet can be identified. As discussed in the reference [32], there are three primary categories, included matrix crushing, fiber breaking and delaminated at the interface between the SMA and matrix. However, the SMA wire near the crushed and delaminated matrix is found relatively intact and protect the left side face-sheet very well. The face-sheet of the SMA hybrid sandwich panel is divided into the crushed and intact parts at the line of SMA wire location. According to the failure shown in SEM figure, the crack and crushed matrix extend along with the interface between SMA wire and matrix. Thus, the embedded SMA wire pre-

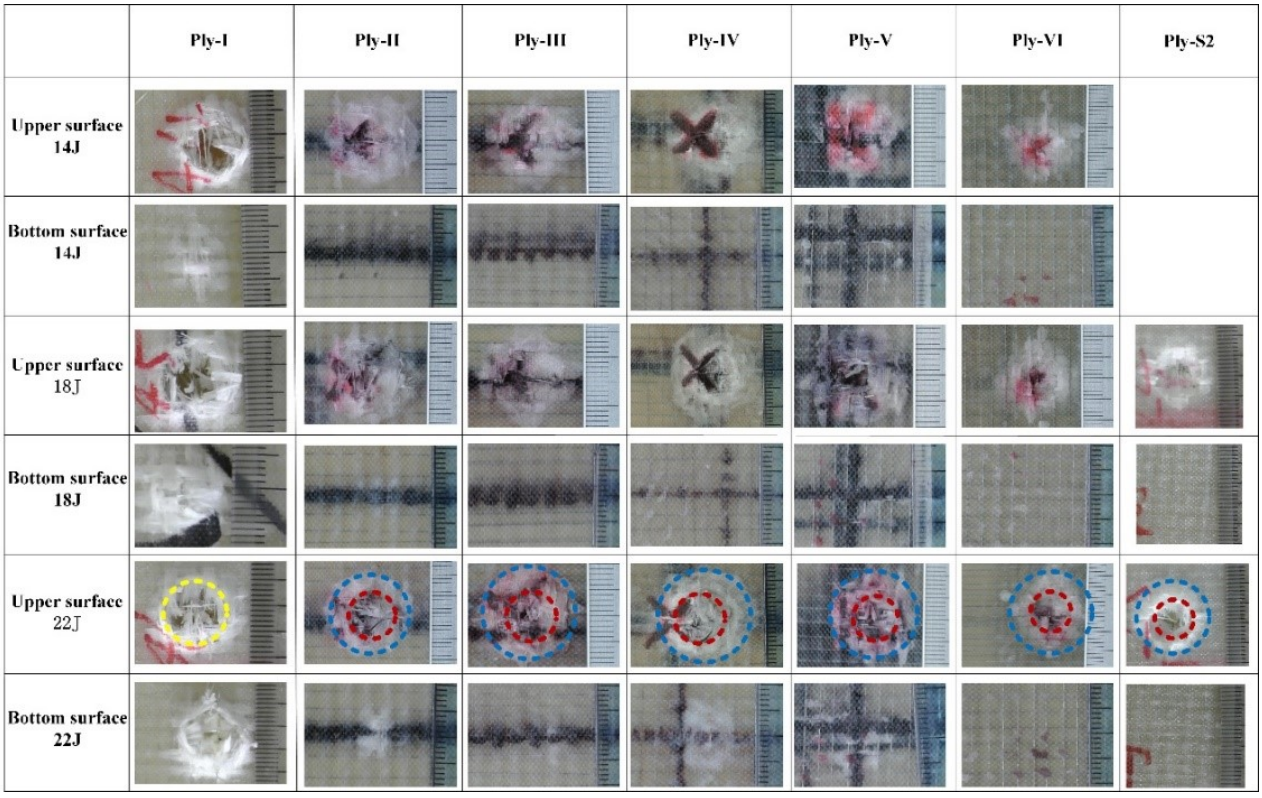

Figure 8: Typical damage morphology of front and rear surfaces of the sandwich panels. Note: Yellow circle with the same diameter as the impactor; Red and blue circle are marked to distinguish complete damage, incomplete failure and intact region.

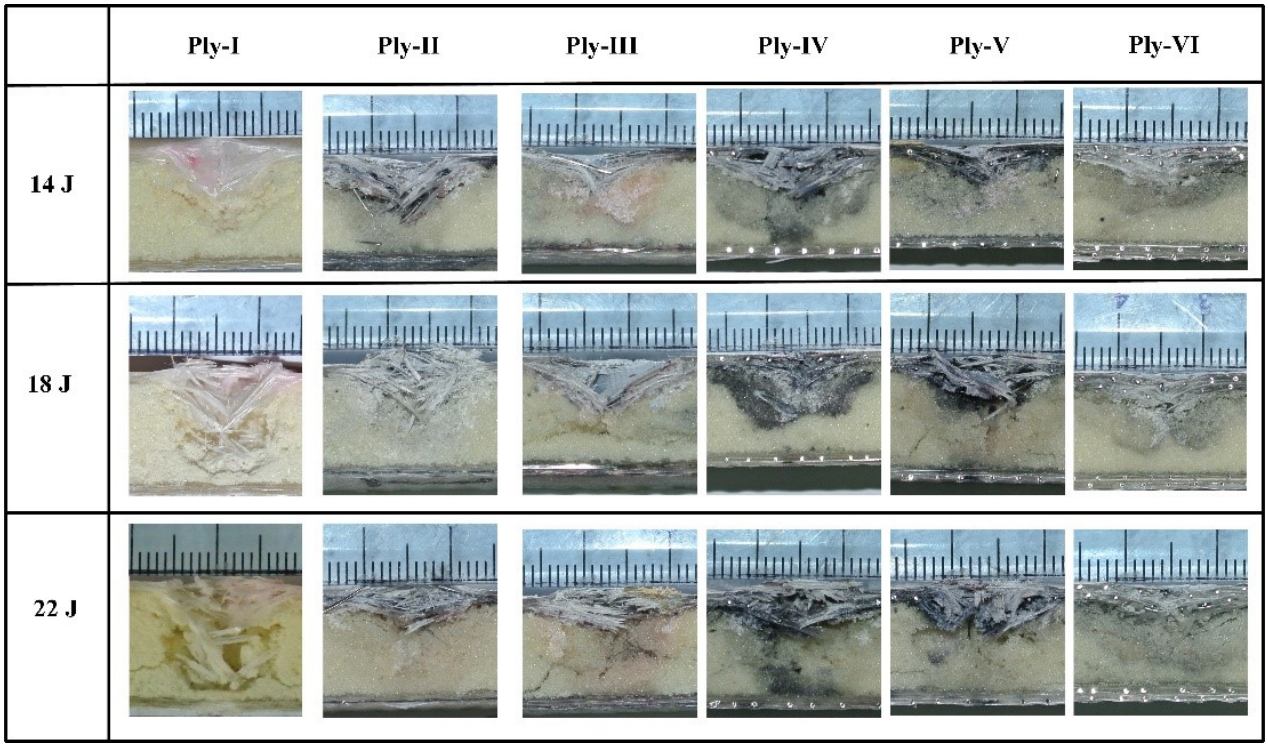

Figure 9: Typical transverse failure models of the central impact regions in the sandwich panels with different ply codes

Table 2: The CAI failure strain u (%) and stress σ (MPa) of different sandwich panels

Incident	Ply I		Ply II		Ply III		Ply IV		Ply V		Ply VI		PlyS2	
Energy	u	σ	u	σ	u	σ	u	σ	u	σ	u	σ	u	σ
0 J	2.065	4.063	1.226	11.726	1.263	17	1.348	15.367	0.949	12.139	1.909	18	0.908	8.489
18 J	0.646	1.39	0.331	4.123	0.814	9.958	1.055	7.393	1.051	2.359	1.103	11.001	0.622	8.036
22 J	0.607	1.45	0.524	2.384	0.743	4.101	0.695	3.615	0.629	2.052	1.243	5	1.397	5.182

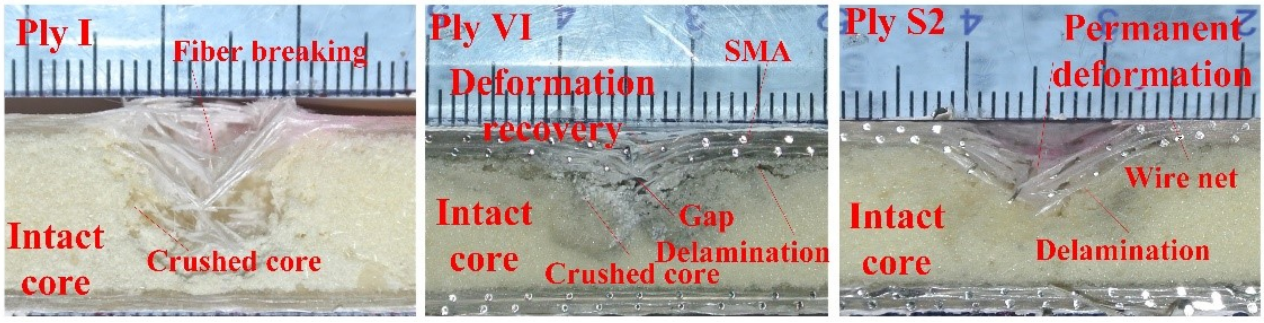

Figure 10: Typical transverse fracture morphology of Ply I, VI and S2 for the incident energy of 18 J

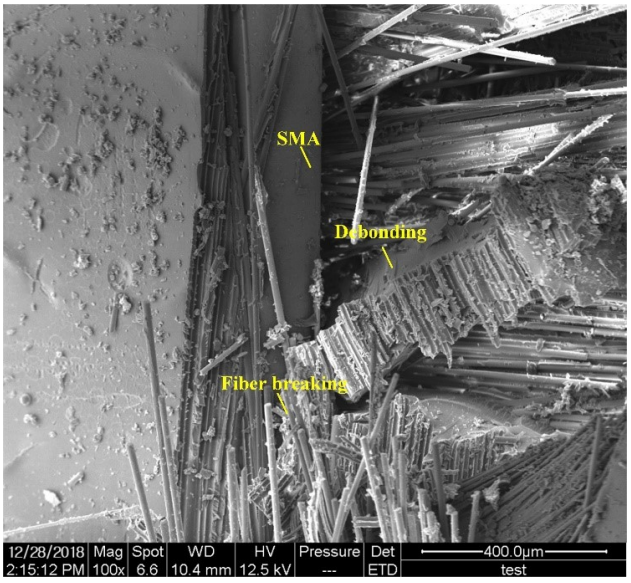

Figure 11: Typical microstructure damage around the impact region of the SMA hybrid sandwich panels

vents the growth of cracks from propagating along the line of SMA wire location. Combining the analysis based on Figure 10, it indicates that when the matrix crack and crushing reach the interface it turns into the direction along the SMA wire during the impact event.

3.3 CAI behavior of different types model of sandwich panels

In the incident energy range from 18J-22J, penetrate and unpenetrated cases were both found in the low-velocity impact test. And, the effect of low-velocity impact on the compressive behavior could presented more clearly. The stress-strain curves of different CAI tests for various impact energies of 0 J, 18 J and 22 J, respectively, are shown in Figure 12. Experimental results show that all the CAI stress firstly increases linearly with strain, and then increases gently. The failure strain and stress of different sandwich panels in CAI tests are summarized in Table 2. For both damaged and undamaged sandwich panels, the failure stress of Ply-VI panels is maximum. Compared with reference Ply I, the compressive strength of Ply-VI undamaged, impact energy of 18 J and 22J increase by up to 3.43, 13.36 and 2.45 times. Based on the results, sandwich panels with two layers of cross SMA wires has better CAI performance. Moreover, for Ply-III, IV and V, they all have two layers of unidirectional SMA wires, and perform better than Ply-I & II in CAI performance. Besides, the Ply-III & IV panels reach higher ultimate compressive stress. Based on the transverse fracture morphology shown in Figure 9, this is due to a lower level of damage for Ply III & IV under the same incident energy. The linear fitting curves of CAI strength versus impact energy for different sandwich panels are shown in Figure 13. As seen in the figure, the compressive strength of all cases decreases with the increasing of impact energy. According to the rate of decrease compressive strength from quickly to slowly, the order is Ply-II-VI, Ply-S2 and Ply-I

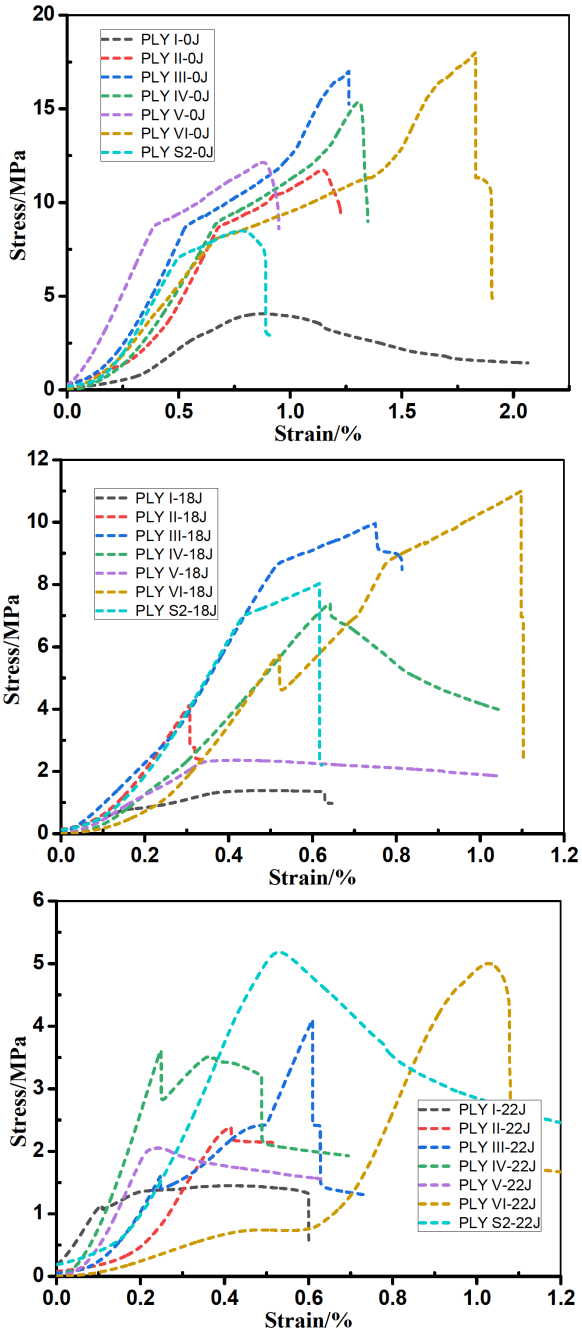

Figure 12: Typical stress-strain curves in compression test after incident energies, 0 J, 18J and 22 J, respectively

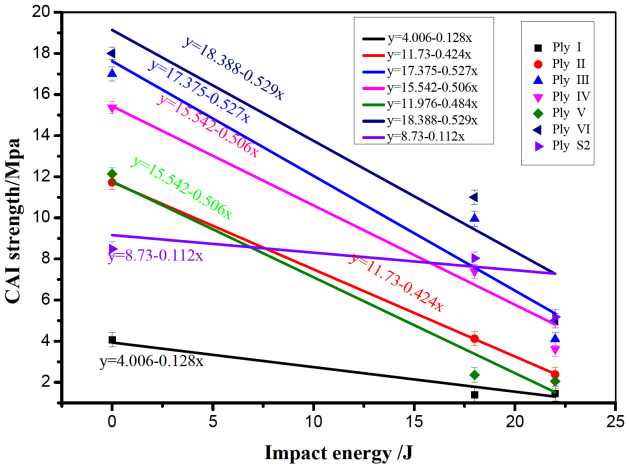

Figure 13: The linear fitting curves of CAI strength versus impact energy for different sandwich panels

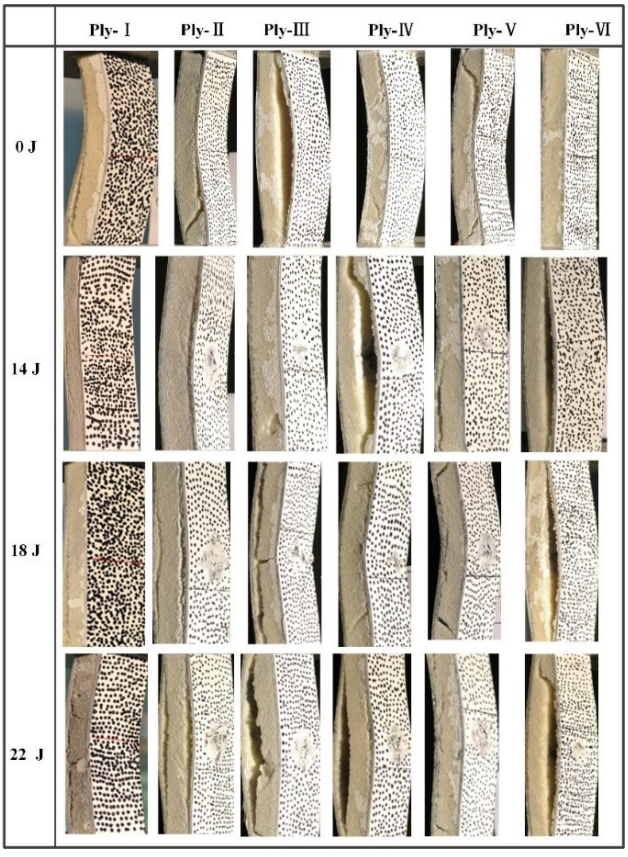

Figure 14: Failure mode of different sandwich panels at CAI test

successively. Thus, the compressive strength of sandwich panels embedded with SMA wires is sensitive to the low-velocity impact load. Combined with the typical failure modes shown in Figure 10, this result is caused by the relatively wider matrix crush in the upper face-sheets. When the impact energy increases greater than 18 J, the CAI result of Ply-I shows a close value, which is because that the upper and bottom face-sheet of sandwich panels are penetrated and there is no big difference in the degree of damage.

Comparison of visual inspection of failure in the CAI tests are shown in Figure 14 & 15. The sandwich panels embedded with nothing shows an overall buckling, while the sandwich panels with more rigid face-sheets embedded

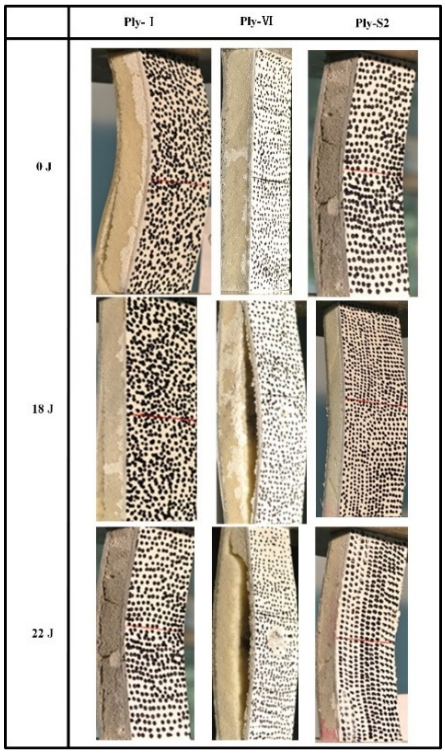

Figure 15: Comparison of failure mode between the sandwiches hybrid with SMA wire and 304 SS wire net

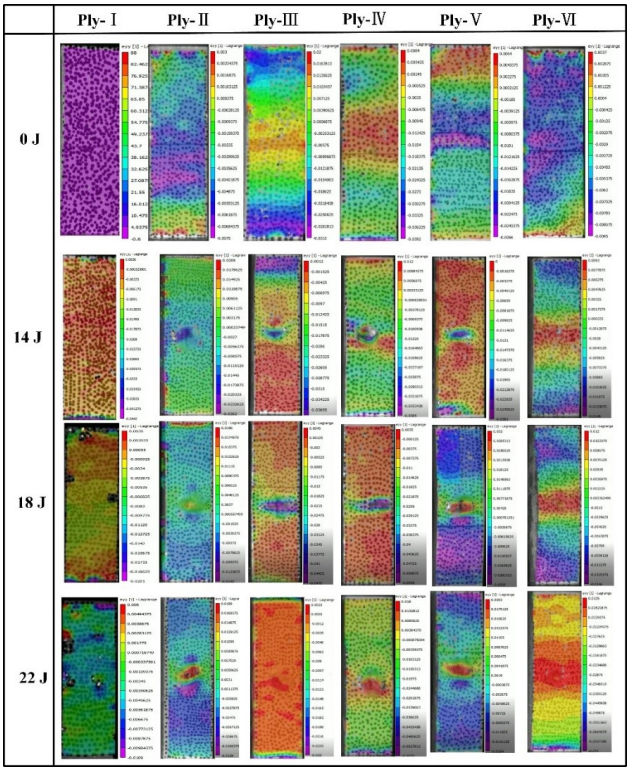

Figure 16: DIC failure mode of different sandwich code at CAI test

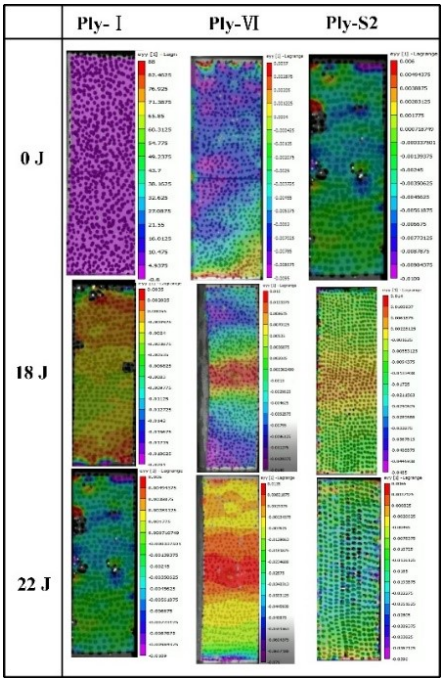

Figure 17: Comparison of DIC image at failure between the sandwiches hybrid with SMA wire and 304 SS wire net

with SMA or 304 SS wire fails with obvious delamination. Generally, delamination formation occurs at the interface between the form core and impaired face-sheet during the CAI event. Besides, as the propagation of interface delamination, the sandwich panels suffers irreversible damage and lose the carrying capacity of compression. This is because there is an already existing damage on the face-sheet and interface which are unstable. During the CAI process, the sandwich panels loses the carrying capacity of compression completely when the delamination reaches any side of the loading plate. DIC failure modes of the different sandwich are shown in Figure 16 & 17. As seen in the figures, all maximal strain along the load direction of the damage sandwich panels is located at the central region. It indicates that the low-velocity impact on the sandwich panels leads to the face-sheet week and this region fails firstly during the CAI test.

4 Conclusion

This study focuses on the low-velocity impact and compression-after-impact (CAI) performance of foam core sandwich panels incorporated with shape memory alloy (SMA) or 304 SS wires. The comparison of failure modes is also presented and discussed. Some conclusions can be drawn as follows:

(a) After inserting superelastic SMA into the GFRP, the impact resistance performance can be improved up to 40.1%. The contact force of hybrid sandwich keeps a large level for a longer time than the sandwich panel with GFRP face-sheets and the sandwich panels embedded with 304 SS wire. Moreover, the sandwich panels embedded with SMA wires of cross configuration could dissipate more impact energy.
(b) Due to the property of super-elasticity, the addition of SMA wires can dissipate and transfer the kinetic energy of impactor to the outer region of the upper face-sheet, which leads to a better impact resistance performance of the sandwich panels embedded with SMA.
(c) In terms of both damaged and undamaged sandwich panels, the failure stress of Ply-VI panels showed maximum value. Compared with the reference Ply I, the compressive strength after impact increases up to 3.43, 13.36 and 2.45 times for the Ply-VI sandwich panels impacted by 0J, 18J and 22J, respectively.
(d) During CAI test, the delamination of the sandwich panels between the foam core and the face-sheet first occur at the impact region. With the propagation of interface delamination, the sandwich panels suffer irreversible damage and lose the carrying capacity of compression. Besides, the DIC results show that the maximum strain is located at the damaged region of the face-sheet.

Acknowledgement: This work was supported by Foundation of Jiangxi Province of China Educational Committee (GJJ180956, GJJ161120, GJJ170395), National Natural Science Foundation of China (51868049, 51609114), Key Research & Development Plan of Jiangxi Province of China (20171BBE50024) and Jiangxi Province Science Foundation (20133BBE50044, 20144BAB2160009, 20181BAB206040).

References

[1] Mangalgiri PD. Composite materials for aerospace applications. B. Mater. Sci. 1999, 22, 657-664.
[2] Schneider C, Kazemahvazi S, Russell BP, Zenkert D, Deshpande VS. Impact response of ductile self-reinforced composite corrugated sandwich beams. Composites Part B: Engineering. 2016, 99, 121-131.
[3] Ascione F. Influence of initial geometric imperfections in the lateral buckling problem of thin walled pultruded GFRP I-profiles. Compos. Struct. 2014, 112, 85-99.
[4] Liu L, Feng H, Tang H, Guan Z. Impact resistance of Nomex honeycomb sandwich structures with thin fibre reinforced polymer facesheets. J. Sandw. Struct. Mater. 2016, 20, 531-552.
[5] Zhou J, Liu J, Zhang X, et al. Experimental and numerical investigation of high velocity soft impact loading on aircraft materials. Aerosp. Sci. Technol. 2019, 90, 44-58.
[6] Yazdani Sarvestani H, Mirkhalaf M, Akbarzadeh AH, Backman D, Genest M, Ashrafi B. Multilayered architectured ceramic panels with weak interfaces: energy absorption and multi-hit capabilities. Mater. Design. 2019, 167, 107627.
[7] Abrate S. Localized impact on sandwich structures with laminated facings. Applied Mechanics Reviews. 1997, 50, 69-82.
[8] Xiao D, Chen X, Li Y, Wu W, Fang D. The structure response of sandwich beams with metallic auxetic honeycomb cores under localized impulsive loading-experiments and finite element analysis. Mater. Design. 2019, 176, 107840.
[9] Gao Q, Ge C, Zhuang W, Wang L, Ma Z. Crashworthiness analysis of double-arrowed auxetic structure under axial impact loading. Mater. Design. 2019, 161, 22-34.
[10] Yang B, Wang Z, Zhou L, Zhang J, Tong L, Liang W. Study on the low-velocity impact response and CAI behavior of foam-filled sandwich panels with hybrid facesheet. Compos. Struct. 2015, 132, 1129-1140.
[11] Ji G, Ouyang Z, Li G. Debonding and impact tolerant sandwich panel with hybrid foam core. Compos. Struct. 2013, 103, 143-150.
[12] Sun XC, Hallett SR. Failure mechanisms and damage evolution of laminated composites under compression after impact (CAI): Experimental and numerical study. Composites Part A: Applied Science and Manufacturing. 2018, 104, 41-59.
[13] Gilioli A, Sbarufatti C, Manes A, Giglio M. Compression after impact test (CAI) on NOMEX™ honeycomb sandwich panels with thin aluminum skins. Composites Part B: Engineering. 2014, 67, 313-325.
[14] Giannopoulos IK, Theotokoglou EE, Zhang X. Impact damage and CAI strength of a woven CFRP material with fire retardant properties. Composites Part B: Engineering. 2016, 91, 8-17.
[15] Rozylo P, Debski H, Kubiak T. A model of low-velocity impact damage of composite plates subjected to Compression-After-Impact (CAI) testing. Compos. Struct. 2017, 181, 158-170.
[16] Sevkat E, Liaw B, Delale F. Drop-weight impact response of hybrid composites impacted by impactor of various geometries. Materials & Design (1980-2015). 2013, 52, 67-77.
[17] Bunea M, Cîrciumaru A, Buciumeanu M, Bîrsan IG, Silva FS. Low velocity impact response of fabric reinforced hybrid composites with stratified filled epoxy matrix. Compos. Sci. Technol. 2019, 169, 242-248.
[18] Caminero MA, García-Moreno I, Rodríguez GP. Damage resistance of carbon fibre reinforced epoxy laminates subjected to low velocity impact: Effects of laminate thickness and ply-stacking sequence. Polym. Test. 2017, 63, 530-541.
[19] Liu H, Falzon BG, Tan W. Experimental and numerical studies on the impact response of damage-tolerant hybrid unidirectional/woven carbon-fibre reinforced composite laminates. Composites Part B. 2018, 136, 101-118.
[20] Li L, Sun L, Wang T, Kang N, Cao W. Repeated low-velocity impact response and damage mechanism of glass fiber aluminium laminates. Aerosp. Sci. Technol. 2019, 84, 995-1010.
[21] Ding Y, Kusterle W. Comparative study of steel fibre-reinforced concrete and steel mesh-reinforced concrete at early ages in panel tests. Cement Concrete Res. 1999, 29, 1827-1834.
[22] Cengiz O, Turanli L. Comparative evaluation of steel mesh, steel fibre and high-performance polypropylene fibre reinforced

shotcrete in panel test. Cement Concrete Res. 2004, 34, 1357-1364.
[23] Liu Z, Liu J, Wu C, et al. Experimental and numerical study of reactive powder concrete reinforced with steel wire mesh against projectile penetration. Int. J. Impact Eng. 2017, 109, 131-149.
[24] Shariyat M, Niknami A. Layerwise numerical and experimental impact analysis of temperature-dependent transversely flexible composite plates with embedded SMA wires in thermal environments. Compos. Struct. 2016, 153, 692-703.
[25] Khalili S, Saeedi A. Dynamic response of laminated composite beam reinforced with shape memory alloy wires subjected to low velocity impact of multiple masses. J. Compos. Mater. 2017, 52, 1089-1101.
[26] Eslami-Farsani R, Khazaie M. Effect of shape memory alloy wires on high-velocity impact response of basalt fiber metal laminates. J. Reinf. Plast. Comp. 2018, 37, 300-309.
[27] Yuan G, Bai Y, Jia Z, Lau K, Hung P. Structural deformation performance of glass fiber reinforced polymer composite beam actuated by embedded indented SMA wires. Composites Part B. 2019, 159, 284-291.
[28] Li H, Liu J, Wang Z, Yu Z, Liu Y, Sun M. The Low Velocity Impact Response of Shape Memory Alloy Hybrid Polymer Composites. Polymers-Basel. 2018, 10, 1026.
[29] Tuo H, Lu Z, Ma X, Zhang C, Chen S. An experimental and numerical investigation on low-velocity impact damage and compression-after-impact behavior of composite laminates. Composites Part B: Engineering. 2019, 167, 329-341.
[30] Wang J, Li J, GangaRao H, Liang R, Chen J. Low-velocity impact responses and CAI properties of synthetic foam sandwiches. Compos. Struct. 2019, 220, 412-422.
[31] Wang J, Li J, GangaRao H, Liang R, Chen J. Low-velocity impact responses and CAI properties of synthetic foam sandwiches. Compos. Struct. 2019, 220, 412-422.
[32] Shipsha A, Zenkert D. Compression-after-Impact Strength of Sandwich Panels with Core Crushing Damage. Appl. Compos. Mater. 2005, 12, 149-164.